# PLASMONIC WAVEGUIDES FEATURES CORRELATED WITH SURFACE PLASMON RESONANCE PERFORMED WITH A LOW REFRACTIVE INDEX PRISM

Georgiana C. VASILE[1], Aurelian A. POPESCU[2] , Mihai STAFE[1], S.A. KOZIUKHIN[3], Dan SAVASTRU[2], Simona DONȚU[2], L. BASCHIR[2], V. SAVA[4], B. CHIRICUȚĂ[4], Mona MIHĂILESCU[1], Constantin NEGUȚU[1], Niculae N. PUȘCAȘ[1]

*The surface plasmon resonance calculations were performed for Kretschmann configuration. Two of the layers, gold and chalcogenide films (GaLaS), have finite thickness. The refractive index of coupling prism material is supposed to be lower than the refractive index of amorphous film which composes a plasmonic waveguide. The amorphous film thickness for which plasmonic resonances occur was established. The calculations were performed for TE- and TM- modes (both for visible and IR domain) concerning the propagation constants, the attenuation coefficient and the electromagnetic field distribution. The results provide the conditions for design an optical memory device based on light-light interaction in plasmonic configuration.*

**Keywords:** plasmonics, photonics, chalcogenide amorphous materials, GaLaS

## 1. Introduction

The plasmons concept was introduced since the beginning of the XXth century as an interaction of electromagnetic waves with the plasma electrons from solid materials (mainly metals) which contain free electrons. Sommerfeld (1899) and Zenneck (1907) have explained the confined propagation phenomenon of electromagnetic waves on the metals surface. The phenomenon analysis was dedicated to wireless telegraph operation, operation based on low frequency radio waves.

In the optical band the confinement of electromagnetic waves at dielectric-metal interface was explained by E. Kretschmann and H. Raether [1] in 1968, who have proposed and experimentally realized a new excitation way of the surface

[1] University POLITEHNICA of Bucharest, Physics Department, Splaiul Independentei, 313, 060042, Bucharest, Romania
Corresponding authors: A.A. Popescu: apopescu@inoe.ro, M. Stafe: stafe@physics.pub.ro,
[2] National Institute R&D of Optoelectronics, INOE 2000, 409 Atomistilor str., PO BOX MG. 5, 77125 Magurele, Ilfov, Romania
[3] Kurnakov Institute of General and Inorganic Chemistry RAS (Russia, Moscow), Leninsky prospect 31, Moskow, 119991, Russia
[4] S.C. Apel Laser SRL, Vintila Mihailescu Str, No. 15, Bl. 60, Sc. 1, Et. 1, Ap. 12, Sect. 6, Bucharest, Romania

plasmons using evanescent waves which form in total reflection conditions or prism method. Confinement of light propagation is obtained on the metal-air interface of the metal film deposed on the prism, when the light is directed on the prism at a resonance angle. The theoretical model used by these authors study a single interface of two semi-infinite media and is based on solving of the Maxwell equations in transverse-magnetic (TM) and transverse-electric (TE) cases and applications of continuity conditions [2].

This analysis leads to the dispersion equation $\omega(k)$ for the surface plasmon-polariton. The examination of the dispersion equation obtained in this case can provide several conditions necessary to realize the confinement of light: a) the incident light on the prism must be polarized in the incidence plane called transverse magnetic (TM); b) dielectric constant (real part) of the film must be negative; c) the dielectric constant of the metal must exceed the dielectric constant of the material which is in contact with the film. This material is usually the ambient (air) or dissolved substances in water. Due to the tight confinement of light on the metal film surface, this configuration has found many applications in developing of some optoelectronics sensors based on plasmon resonance [3-5]. As was demonstrated earlier, the surface plasmon resonance (SPR) is very sensitive, up to $10^{-4}$ - $10^{-5}$ changes of the refractive index. The excellent results were obtained in plasmon resonance applications as biosensors [6, 7].

A new direction in the surface plasmon resonance applications consists in the deposition on the metal surface of a dielectric film whose properties can be changed by applying an electric field, illumination s.a. In the chalcogenide glasses (ChG) changes of the optical constants arise under the action of light with the photon energy exceeding the band gap. Stationary and dynamic photoinduced absorption may be distinguished [8]. The modifications of the optical absorption correlate with the modifications of the refractive index by Kramers–Kronig relation. However, the change of the refractive index in chalcogenide films is small, on the order of $10^{-3}$, and a sensitive experimental method has to be used. The surface plasmonic resonance is an opportunity to develop new devices. In a recent investigation the authors [9] proposed and have experimentally demonstrated the SPR configuration light modulation by use of thin GaLaS chalcogenide light sensitive amorphous which is deposited on top of silver film with the thickness of 30-50 nm. In order to satisfy plasmonic resonance conditions they use a $TiO_2$ high refractive index prism. Using the transfer matrix formalism, in [10] have been elucidated several resonance angles in SPR structure which contain a metallic and amorphous chalcogenide films with high refractive index ($n = 2.47$), typical for GaLaS or $As_2S_3$ compounds. In this paper the case of GaP prism with refractive index higher ($n = 3.3$) was examined. The results are explained by coupling of evanescent wave with plasmonic waveguide modes.

The need to use the high refractive index materials for the prism manufacture limits the type of usable materials. The fulfilling of this condition is necessary if one consider the total excitation spectrum of the modes. The possibility to use the materials with lower refractive index of the prism, for example BK7 glass ($n = 1.51$), for excitation modes of $As_2S_3$ plasmonic waveguide (material with high refractive index) has been established in [11]. In this paper only the numerical simulations results for TE modes were presented. The TM modes have not been examined due to the complex character of the propagation constant and the complex numbers operation.

In the present paper we investigated both TE and TM modes by numerical simulations. We determined the structure parameters for which the coupling of free electromagnetic wave to the confined modes of the planar plasmonic waveguide can be realized.

## 2. The plasmonic waveguide structure with GaLaS chalcogenide film

The typical plasmonic planar waveguide consists of a structure of long and large layers in the plane *yz*. In each region the refractive index may be considered as constant. The constituent regions are as follows:

- a substrate made from oxide glass (BK7) which may be considered semi-infinite;
- a thick enough gold film which have a complex refractive index;
- a dielectric film made of GaLaS which is the waveguide;
- a cover region considered semi-infinite (air).

The model of the structure that carry resonance light coupling in plasmonic waveguide is shown in Fig. 1. Here, $n_m$ denotes the real part of the refractive index of the metallic layer. The refractive indexes of the layers at two wavelengths are given in Table 1. One can see that the optical waveguide layer has the largest index $n_f > n_m > n_a$. According to the matrix calculations, the thickness of the gold film could be around 50 nm in order to achieve 100% *resonant coupling of the incident radiation to the waveguide*.

We may take into account also that due to skin-effect the penetration depth of light in gold is about 20 nm. It means that in visible and near IR spectral domain the metallic film can be considered to be thick enough so as the substrate material didn't significantly alter the waveguide mode spectrum. In the same time the waveguide field may have a weak coupling with evanescent wave on the prism base. Meanwhile the waveguide field may have a weak coupling with the evanescent wave on the prism.

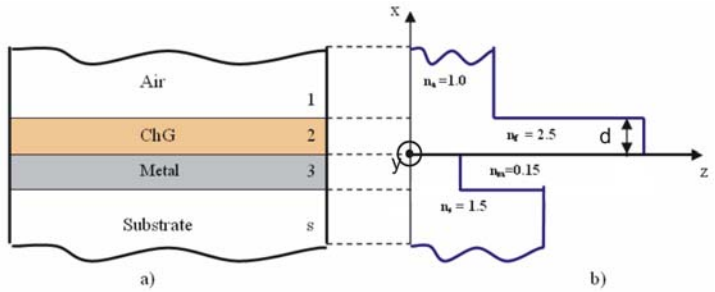


Fig.1. Plasmonic waveguide structure (a) and the reflective index profile (b).

The real value of the complex metal refractive index is presented in Fig. 1(b). The cover (air) and substrate (BK7) regions are much thicker than λ and we consider these regions as semi-infinite. Such an approximation considerably simplifies the form of the dispersion equation and also the finding of solutions in the complex plan. Finally, we will write the electromagnetic field relations for the 3-layer waveguide system as the fields are weakly linked with the prism medium. The parameters values that were used in calculations are shown in the table below.

Table 1. The layers refractive index at two working wavelengths

| No. | Incident laser wavelength (nm) | Air refractive index | GaLaS refractive index [13] | Gold refractive index [12] *) |
|---|---|---|---|---|
| 1. | 633 | 1 | 2.48 | 0.197 - 3.09i |
| 2. | 1310 | 1 | 2.38 | 0.48 - 8.75i |

*) We use the convention (n-iκ) for the complex refractive index as the plane wave below are taken in the form of $e^{[i(\beta z-\omega t)]}$.

The metallic substrate lies in the region x<0 and the air cover lies in the region x>d. The film thickness *d* is varied between 0.1 and 1.6 μm which is comparable to the laser wavelength.

## 3. Light propagation in plasmonic waveguides: numerical simulation for TE-modes case

The electric fields of the propagating TE modes in the three regions can be written as follows:

$$E_{y\_waveguide}(x,z)=(A\cdot e^{ik_2x}+B\cdot e^{-ik_2x})e^{-i\beta z} \tag{1a}$$

$$E_{y\_metalfilm}(x,z)=C\cdot e^{k_3x}\,e^{-i\beta z} \tag{1b}$$

$$E_{y\_cover}(x,z)=D\cdot e^{-k_1(x-d)}\,e^{-i\beta z} \tag{1c}$$

Here, $k_2 = \sqrt{n_2^2 k_0^2 - \beta^2}$ is the transversal wave number within the optical waveguide along the x direction. The wave numbers for the cover and the metallic regions are given by the relations $k_1 = \sqrt{\beta^2 - n_1^2 k_0^2}$ and $k_3 = \sqrt{\beta^2 - n_3^2 k_0^2}$, respectively. $\lambda_0 = 2\pi / k_0 = c/\omega$ is the wavelength of the incident radiation. The propagation constant $\beta$ along the *z* direction is the same in the three layers of the waveguide due to the continuity condition of the electromagnetic field components at the waveguide boundaries. The dispersion equation for the TE modes can be obtained from the continuity conditions of the electric field $E_y$ and of the magnetic field $H_z$ (proportional to the derivative $\partial_x E_y$ of electric field) at the two boundaries of the waveguide. As we are interested to the relative field distribution, we may consider one of the integration constant equal to unity. By excluding the other constants, the following equation may be obtained:

$$e^{-2idk_2} = \frac{(ik_2 + k_1)(ik_2 + k_3)}{(ik_2 - k_1)(ik_2 - k_3)} \tag{2}$$

Taking into account that :

$$\tanh(idk_2) = \frac{1 - e^{-2idk_2}}{1 + e^{-2idk_2}} \text{ and } \tanh(idk_2) = i \cdot \tan(dk_2), \tag{3}$$

the following relation between transverse wave numbers $k_i$ ($i = 1,2,3$) may be obtained:

$$\tan(k_2 d) = \frac{k_2(k_1 + k_3)}{k_2^2 - k_1 k_3} \tag{4}$$

Equation (4) constitutes the dispersion relation $k_i = f(\omega)$. For the convenience of numerical solution, Eq. (4) may be inverted and written in the form:

$$k_2 \cdot d = \arctan\left(\frac{k_1}{k_2}\right) + \arctan\left(\frac{k_3}{k_2}\right) + m\pi \tag{5}$$

In Eqs. (3-5), *m* represents the mode number and *d* is the film thickness, which play the role of parameter. This equation related to lossless waveguides was obtained by Marcuse [14, 15] for the first time. All the wave numbers ware considered as reals. In our case of contrary, the transversal wave number as well as the propagation constant $\beta$ should be considered as complex number and suitable solution methods may be applied.

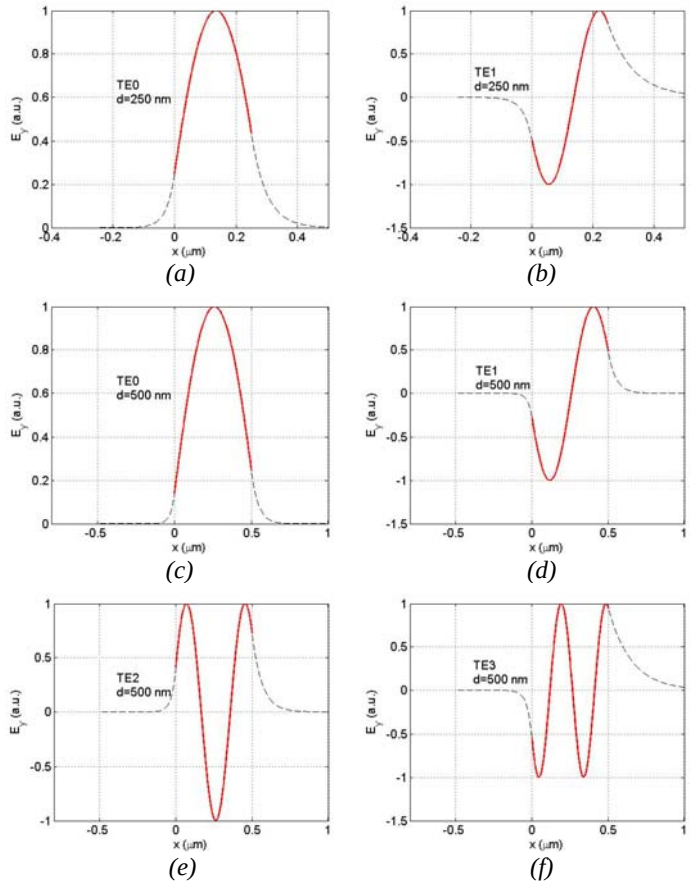


Fig. 2. $E_y$ field of different TE modes across the three regions of the waveguide for a film thickness of 0.25 μm (a, b) and 0.5 μm (c-f) at 633 nm wavelength.

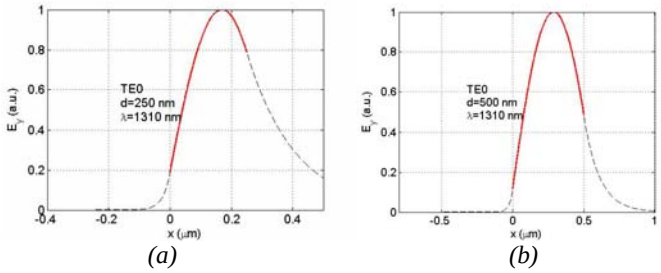

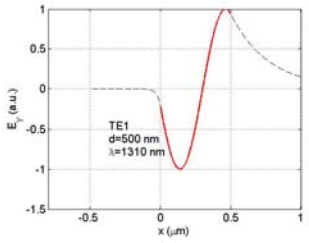


*(c)*

Fig. 3. $E_y$ field of different TE modes across the three regions of the waveguide for a film thickness of 0.25 μm (a) and 0.5 μm (b, c) at 1310 nm wavelength

The numerical solutions of Eq. (5) and the electromagnetic fields in the three regions given by Eq. (1) were determined by using Matlab. The results corresponding to $\lambda_0$=633 nm are presented in Figs. 2, 4 and 6, whereas the results for $\lambda_0$=1310 nm are presented in Figs. 3, 5 and 7. The electric field $E_y$ across the waveguide (i.e. as a function of transverse x direction) for the TE propagating modes at $\lambda_0$=633 nm is given in Figs. 2(a, b) for *d*=0.25 μm, and in Fig. 2 (c-f) for *d*=0.5 μm, respectively. For incident radiation at 1310 nm wavelength, the electric field $E_y$ across the waveguide for the TE propagating modes is given in Figs. 3(a) for *d*=0.25 μm, and in Fig. 3 (b, c) for *d*=0.5 μm. One can observe that the number of propagating modes is two times smaller in case of 1310 nm wavelength as compared to 633 nm radiation.

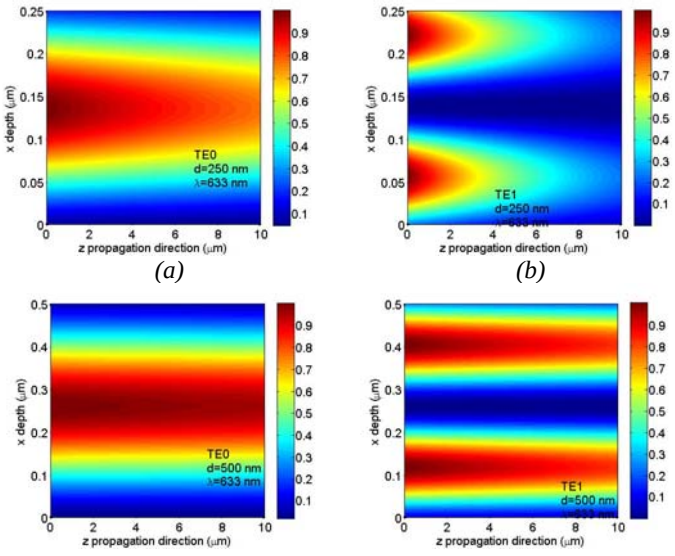


*(a)* *(b)*

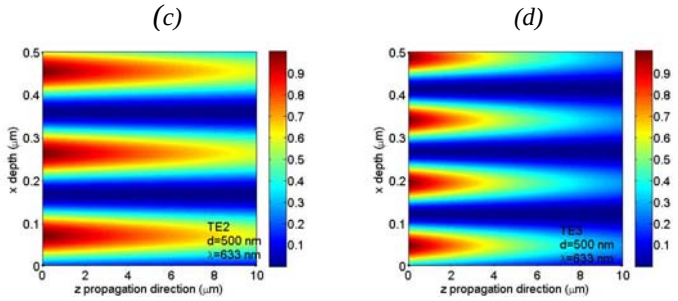


Fig. 4. Intensity of the TE modes in xz section of the waveguide for a film thickness of 0.25 μm (a, b), and 0.5 μm (c-f) at 633 nm wavelength.

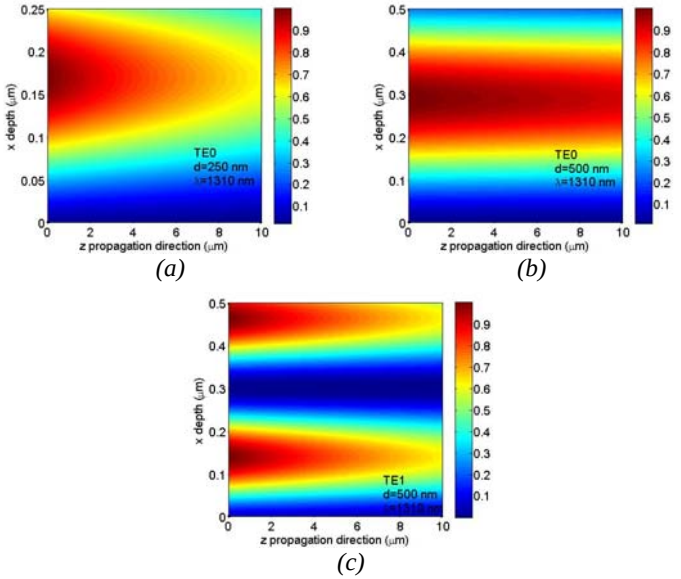


Fig. 5. Intensity of the TE modes in xz section of the waveguide for a film thickness of 0.25 μm (a) and 0.5 μm (b, c) at 1310 nm wavelength.

The light intensity distribution in *xz* cross section of the waveguide for the two propagating modes ($TE_0$ and $TE_1$) in the 0.25 μm waveguide is given in Figs. 4(a, b). The 0.5 μm thick waveguide enables propagation of four TE modes, namely $TE_0$-$TE_3$. The light intensity distribution in *xz* cross section of the waveguide for these modes is given in Figs. 4(c-f). The light intensity distribution in *xz* cross section of the waveguide for the propagating mode ($TE_0$) in the 0.25 μm waveguide is given in Fig. 5(a). The 0.5 μm thick waveguide enables propagation of two TE modes, namely $TE_0$, $TE_1$. The light intensity distribution in *xz* cross section of the waveguide for these modes is given in Figs. 5(b, c).

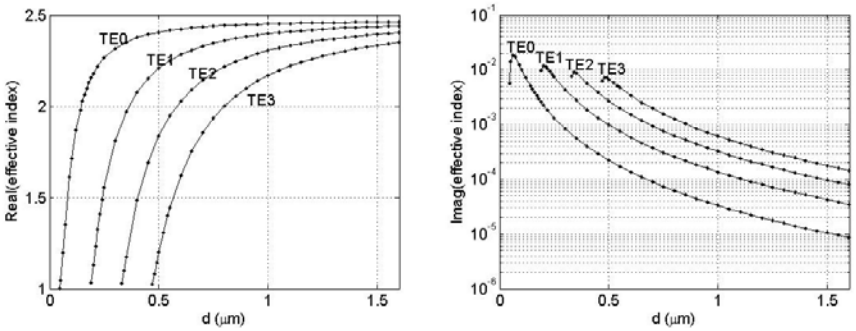


*(a)* *(b)*

Fig. 6. The real (a) and imaginary (b) parts of the effective refractive index as a function of waveguide thickness, for the first four TE modes at 633 nm wavelength.

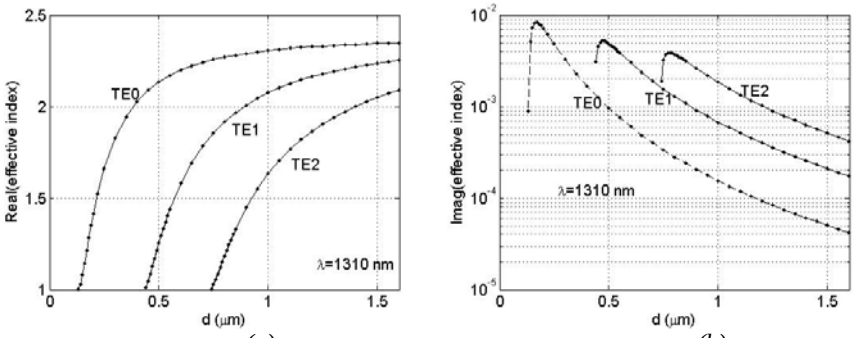


*(a)* *(b)*

Fig. 7. The real (a) and imaginary (b) parts of the effective refractive index as a function of waveguide thickness, for the first three TE modes at 1310 nm wavelength.

Figs. 6 and 7 present the real and imaginary parts of the effective refractive index $\beta/k_o$ of the waveguide as a function of waveguide thickness for different TE modes at 633 nm and 1310 nm wavelength radiation. The dispersion curves in Fig. 6(a) indicate that the 0.25 μm thick waveguide enables propagation of two $TE_0$ and $TE_1$ modes at 633 nm wavelength, whereas Fig. 7(a) indicates that only one mode (i.e. $TE_0$) can propagate at 1310 nm wavelength. A closer analysis of these figures demonstrates that the effective index of the TE modes increases asymptotically from 1 to 2.48 at 633 nm (respectively 2.37 at 1310 nm wavelength), i.e. between the smallest refractive index (the cover's) and the highest refractive index (the film's), when increasing the waveguide thickness.

By analysing the Figs. 6(b) and 7(b) one can see that the attenuation of the propagating modes is stronger for the propagating modes at 1310 nm as compared to 633 nm. For example, for the thicknesses 0.25 and 0.5 μm, the imaginary effective refractive index (which also gives the attenuation coefficient along the *z*

direction) for the $TE_0$ mode is approximately four times smaller at 633 nm than 1310 nm wavelength. This can also be seen in Figs. 4(a) and 5(a).

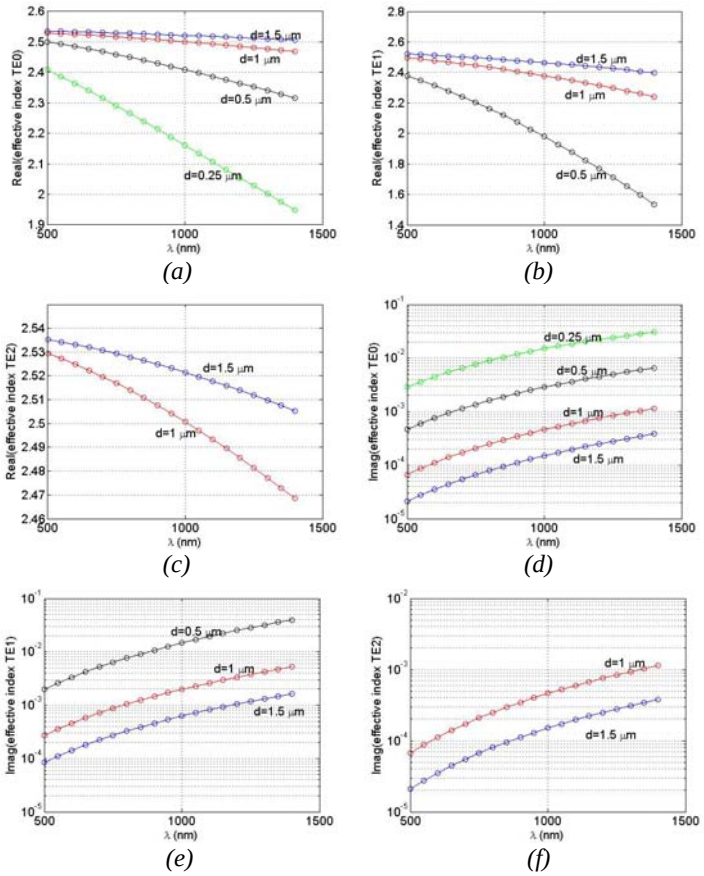


Fig. 8. The real (a-c) and imaginary (d-f) parts of the effective refractive index as a function of incident wavelength, for different propagating TE modes.

The influence of the incident laser wavelength on the propagation of the TE modes in waveguides of different thicknesses is given in Fig. 8. The dependence of refractive indexes $n_2 = n_f$ and $n_3 = n_m$ of the dielectric film and metallic layer on wavelength is taken from [12, 13]. The figure indicates that for the full range of wavelengths under study here (500-1400 nm) the effective index decreases with wavelength. Moreover, the figures demonstrate that the $TE_0$ mode can propagate in waveguides thicker than 0.25 μm (Fig. 8(a)), $TE_1$ mode needs thicknesses larger than 0.5 μm (Fig 8(b)), and $TE_2$ mode needs waveguide thicknesses larger than 1 μm (Fig 8(c)). Figs. 8 (d-f) show that the attenuation of the TE modes along the *z* direction becomes stronger as the wavelength increases.

## 4. Light propagation in plasmonic waveguides: numerical simulation for TM-modes case

The electric fields of the propagating TM modes in the three regions can be written as follows:

$$H_{y\_waveguide}(x,z) = (A \cdot e^{ik_2 x} + B \cdot e^{-ik_2 x}) e^{-i\beta z} \tag{6a}$$

$$H_{y\_metalfilm}(x,z) = C \cdot e^{k_3 x} e^{-i\beta z} \tag{6b}$$

$$H_{y\_cover}(x,z) = D \cdot e^{-k_1 (x-d)} e^{-i\beta z} \tag{6c}$$

The dispersion equation for the TM modes can be obtained from the continuity conditions of the magnetic field $H_y$, and of electric field $E_z$ components at the two boundaries of the waveguide. Performing the same steps as above, the dispersion relation may be obtained:

$$k_2 \cdot d = \arctan\left(\frac{n_2^2}{n_1^2}\frac{k_1}{k_2}\right) + \arctan\left(\frac{n_2^2}{n_3^2}\frac{k_3}{k_2}\right) + m\pi \tag{7}$$

In Eqs. (6,7), $m$ represents the mode number and $d$ is the film thickness. The form of the equation is the same as was obtained in [14] when the media were considered lossless, meaning that the material parameters were considered real. Based on the plasmonic structure presented in Figs. 1 a), b) the numerical simulations were performed in Matlab and some results are presented in Figs. 9, 10, 11 and 12.

The distribution of the magnetic field $H_y$ across the three regions of the waveguide (i.e. the transverse x direction) for the TM propagating modes is given in Figs. 9 (a,b) for $d$=250 nm and in Figs. 9 (c-f) for the 500 nm film thickness, respectively. The metallic film lies in the region $x$<0 and the air cover lies in the region $x$>$d$.

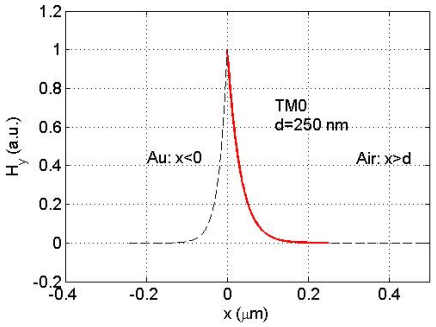


*(a)*

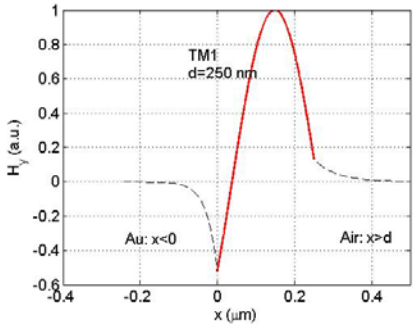


*(b)*

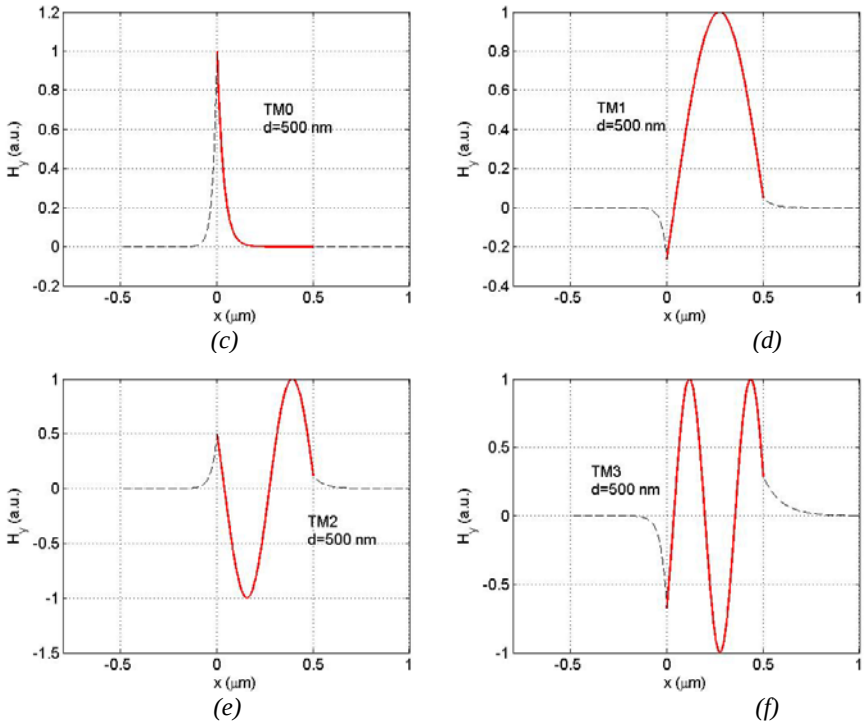


Fig. 9. TM modes for a film thickness (d) of 250 nm (a,b) and 500 nm (c-f)

Figs. 9 (a, c) indicate a sharp spike of the magnetic field of $TM_0$ mode at the film-metal interface. In other words, there is a strong confinement of the mode in ~50 nm thickness of film near the film-metal interface. In fact, $TM_0$ modes correspond to surface wave modes. Thereby, it is expected that the $TM_0$ mode propagation and attenuation to be practically independent of film thickness when thickness is larger than ~100 nm. This is demonstrated in Fig. 10, which presents the real and imaginary parts of the effective refractive index of the waveguide as a function of waveguide thickness for the $TM_0$ mode.

Fig. 10 also indicates that the 250 nm thick waveguide enables propagation of two modes: $TM_0$ and $TM_1$ modes. The light intensity distribution in *xz* cross section of the waveguide for these modes is given in Fig. 11 (a,b). The 500 nm thick waveguide enables propagation of four TM modes, namely $TM_0$-$TM_3$. The light intensity distribution in *xz* cross section of the waveguide for these modes is given in Fig 11 (c-f).

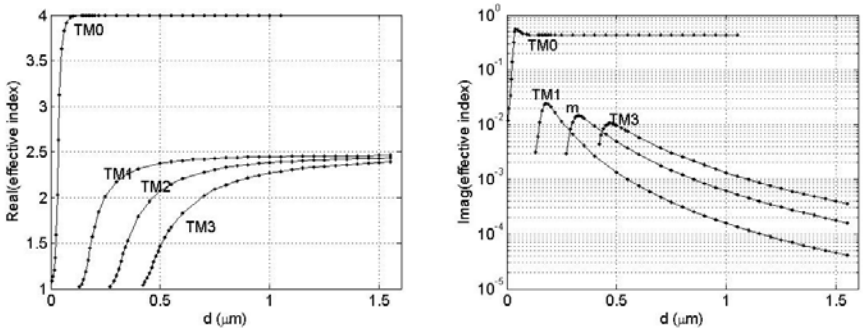


*(a)* *(b)*

Fig. 10. The real (a) and imaginary (b) parts of the effective refractive index as a function of waveguide thickness d, for the first four TM modes.

A closer analysis of Fig 10 a) demonstrates that the effective index of the $TM_1$-$TM_3$ modes increases from 1 to 2.48, i.e. the refractive indices of cover and film. The effective refractive index corresponding to the $TM_0$ modes increases rapidly with film thickness to a value larger than the 2.48. Fig. 10(b) indicates also that the attenuation of the $TM_0$ mode along the z direction is ~ 1 order of magnitude higher than for the other modes. This is consistent with the results presented in Figs. 11 (a,c) which demonstrate the $TM_0$ mode propagate on distances of the order of 400 nm along the z axis, whereas Fig. 11 (b,d-f) demonstrate that the other modes propagate over distances of the order of 4 μm.

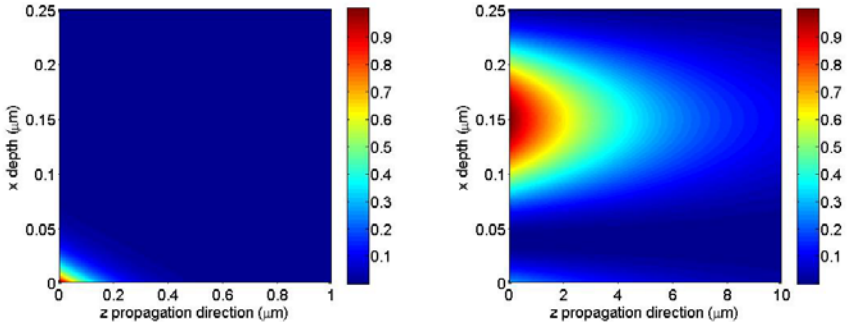


*(a)* *(b)*

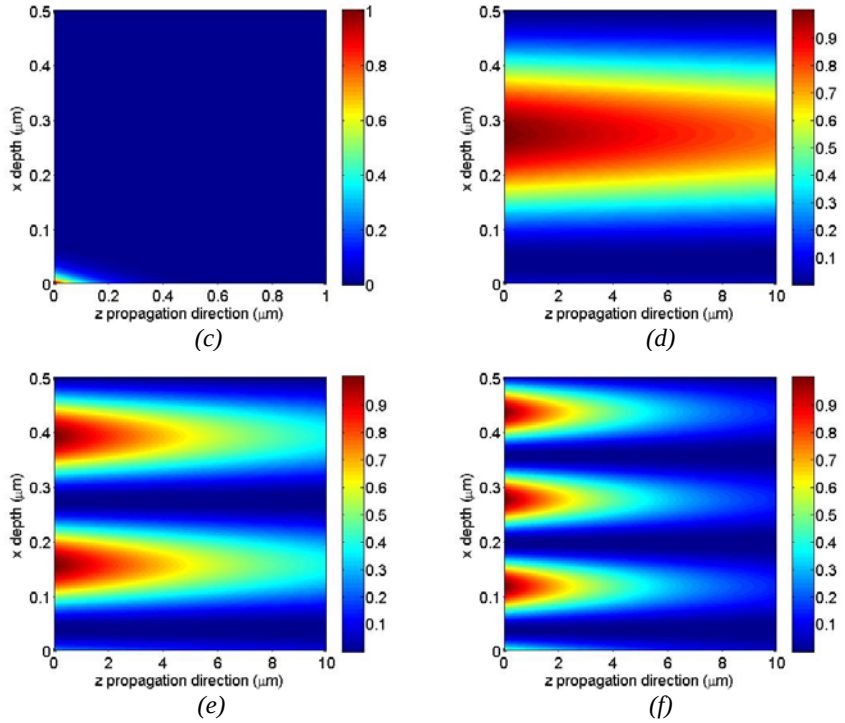


Fig. 11. Intensity in xz section of the waveguide of the TM modes for a film thickness of 250 nm (a,b) and 500 nm (c-f)

## 5. Conclusions

The investigations of the guided modes provided the numerical simulations of plasmonic waveguide structure. The structure is composed by gold film, chalcogenide GaLaS amorphous film of finite thickness and semi-infinite cover, air for instance. The analysis showed the field distributions, attenuation for different mode and effective index value necessary for coupling the light into plasmonic waveguide via prism with low refractive index. For example, the film thickness must be in a narrow region of 120-180 nm (Fig.10) in order to excite $TM_1$ mode. Or, in a narrow band from 180 to 240 nm (Fig. 6) at the wavelength 633 nm for coupling of light into $TE_1$ mode. A space resolution as low as 400 nm may be realized for the $TM_0$ mode. The resolution increases at longer wavelength in the IR region.

**Acknowledgements**.

This work was supported by a grant of the Romanian National Authority for Scientific Research, CNDI – UEFISCDI, project number PN-II-PT-PCCA-2011-25 / 2012.

## R E F E R E N C E S

[1] *Kretschmann, E. and Raether, H.* (1968). Radiative decay of non-radiative surface plasmons excited by light. Z. Naturforschung, 23A: 2135-2136

[2] *Stefan A. Maier*, Plasmonics: Fundamentals and applications, Springer, 2007.

[3] *Sergiy Patskovsky, Andrei V. Kabashin, Michel Meunier, John H.T. Luong*, Near-infrared surface plasmon resonance sensing on a silicon platform, Sensors and Actuators B 97, (2004), 409-414

[4] *Zdzislaw Salamon, H. Angus Macleod,* Gordon Tollin, Surface plasmon resonance spectroscopy as a tool for investigating the biochemical and biophysical properties of membrane protein systems. I: Theoretical principles, Biochimica et Biophysica Acta 1331, (1997), 117-129

[5] *Jirı Homola, Sinclair S. Yee, Gunter Gauglitz*, Surface plasmon resonance sensors: review, Sensors and Actuators B, Vol. **54**, (1999), 3-15

[6] *Yun-Tzu Chang, Yueh-Chun Lai, Chung-Tien Li, Cheng-Kuang Chen, Ta-Jen Yen,* A multi-functional plasmonic biosensor, OPTICS EXPRESS, Vol. **18**, No. 9, (2010), 9561-9569

[7] *Rajan Jhaa, Anuj K. Sharmab*, Design of a silicon-based plasmonic biosensor chip for human blood-group identification, Sensors and Actuators B Vol. **145**, (2010), 200-204

[8] *J. Orenstein, M. Kastner*, Photocurrent Transient Spectroscopy: Measurement of the Density of Localased States in a-$As_2S_3$, Phys. Rev. Lett. Vol. **46,** (1981), 1421-1424

[9] *Zsolt L. Sámson, Shih-Chiang Yen, Kevin F. MacDonald, Kenton Knight, Shufeng Li, Daniel W. Hewak, Din-Ping Tsai, Nikolay I. Zheludev*, Chalcogenide glasses in active plasmonics, Phys. Status Solidi RRL, Vol. **4**, (2010), 274-276,

[10] *A.A. Popescu, R. Savastru, D. Savastru, S. Miclos,* Application of vitreous as-s-se chalcogenides as active layer in surface plasmon resonance configuration , Digest journal of nanomaterials and biostructures, Vol. **6**, no 3, (2011) , 1245-1252

[11] *Georgiana C.Vasile, Roxana Savastru, A.A. Popescu, M. Stafe,D. Savastru, Simona Dontu, L. Baschir, V. Sava, B. Chiricuta, M. Mihailescu, C. Negutu and N.N. Puscas*, Modelling The 2d Plasmonic StructuresWith Active Chalcogenide Glass Layer, Romanian Reports in Physics, Vol. **65**, No. 3, (2013), 1012–1018

[12] *Edward D. Palik*, Handbook of Optical Constants of Solid, Academic Press, Boston, 1985.

[13] *Marvin J. Weber*, Handbook of Optical Materials, CRC PRESS, 2003.

[14] *D. Marcuse*, Coupling Coefficients For Imperfect Asymmetric Slab Waveguides, Bell Syst. Tech. J., Vol. **52**, (1973), 63-82

[15] *D. Marcuse*, Theory of dielectric optical waveguides, Second ed., Academic Press, Inc., 1991